JMEPEG (2017) 26:4522–4532
DOI: 10.1007/s11665-017-2909-y

1059-9495/$19.00

On Mechanical Properties of Graphene Sheet Estimated Using Molecular Dynamics Simulations

D.K. Das and M.M. Ghosh

(Submitted October 25, 2016; in revised form June 2, 2017; published online September 1, 2017)

This work reports estimation of mechanical properties, particularly Young's modulus of a single-layered graphene sheet by molecular dynamics (MD) simulation-based four different approaches, viz. tensile modeling, bending modeling, oscillation modeling and equilibrium MD modeling. The Young's modulus is estimated to be of the order of some TPa. The equilibrium MD method has yielded a Young's modulus value lower than the other non-equilibrium methods, due to the absence of any external forcing factor. Among the non-equilibrium MD methods, the bending modeling is found to predict the highest value of Young's modulus. Comparison among different non-equilibrium methods has established the effect of strain rate on the estimated value of the Young's modulus. The MD simulation-based approaches adopted here can be useful for the design of graphene and graphene-based materials in advanced mechanical applications.

Keywords graphene, mechanical properties, molecular dynamics

1. Introduction

Graphene, the single-layered crystalline form of carbon which is arranged in a two-dimensional honeycomb lattice, has many potential applications in diverse sectors and hence has attracted intense research interest in the current decade. Hexagonally arranged carbon atoms with sp^2 hybridization form both sigma (σ) and pi (π) bonds in graphene. Apart from its very high yield strength and Young's modulus, graphene also possesses very high electrical and thermal conductivity due to the pi (π) bond in it. The presence of this π bond in graphene is also the cause of its lubricating nature (Ref 1). Qi et al. have established very high strength and lots of potential mechanical and structural applications of graphene (Ref 2). Graphene is proved to be the strongest (tensile fracture strength of ~130 GPa) and stiffest (Young's modulus of ~1 TPa) material. Its thermal conductivity (~5000 W m^{-1} K^{-1}) is the highest among the materials discovered so far. Owing to its remarkable mechanical and thermal properties, graphene can be a potential filler material for copper-based nanocomposites to be used in advanced mechano-thermal applications, such as thermal management systems in advanced electronic devices (Ref 3, 4). Graphene is stronger than diamond, more conductive than copper and more flexible than rubber (Ref 5).

Lavoisier (Ref 6) coined the term "Carbone" in his book "Traite Elementire de Chimie" as one of the newly identified chemical elements sometime around 220 years back. He also pointed out the versatility of carbon (as it is now called) and showed that it has variety of forms like diamond, graphite. (Ref 6). Graphene is recently discovered carbonaceous 2D material having crystalline structure and promising mechanical and physical properties, which mostly supersede those of the conventional materials. Since its discovery by Geim and Novoselov (Ref 7), it is proved to be a miraculous material for different advanced applications. Carbon is the only material which exists as four different dimensions, viz. 0D, 1D, 2D and 3D. Graphene is the first 2D atomic crystal available to us. A large number of material properties like mechanical stiffness and strength, electrical and thermal conductivity and many other properties are extraordinary in graphene (Ref 7, 8). Because of these superior properties, graphene can replace other materials in advanced applications. All these properties combined in graphene would likely to give rise to several disrupted technologies. Graphene has diverse type of applications because of its several encouraging properties. It can potentially be used as reinforcing material in nanocomposites to be used in advanced structural applications (Ref 2). The combination of transparency, conductivity and elasticity in graphene makes it suitable for flexible electronics, whereas transparency, impermeability and conductivity of graphene may be useful for transparent protective coatings and barrier films (Ref 8).

The mechanical properties of graphene, particularly Young's modulus, yield strength, tensile strength and Poisson's ratio, have been studied both theoretically and experimentally and are found to be much superior than conventional materials used in engineering sectors nowadays. In one experimental study, the value of Young's modulus of single-walled graphene sheet was reported to be 1.034 TPa (Ref 9). Lee et al. (Ref 10) have found this value to be 2.4 TPa. It is said that graphene is more than 100 times stronger than steel (Ref 11). The tensile strength of graphene has also been evaluated and is found to be ~130 GPa (Ref 9, 12). Liu et al. (Ref 13) have found a Young's modulus value of 1.05 TPa of graphene sheet at a small strain, by using ab initio method of calculation. The values of Young's modulus and Poisson's ratio of graphene sheets, reported in some literatures, are in the range of 1.01 to 1.272 TPa and 0.14 to 0.21, respectively (Ref 14-16). It is to be noted here that the majority of experimental studies reported in the literatures are based on using a collection of numerous graphene sheets of varying sizes, since a single graphene sheet is not accessible

D.K. Das and **M.M. Ghosh**, Department of Metallurgical and Materials Engineering, National Institute of Technology, Durgapur West Bengal 713209, India. Contact e-mail: mmgnitd@gmail.com.

under the measurement device. This is a possible source of some error. The measured value would have been more accurate had it been based on a single graphene sheet. However, simulations can be carried out easily using individual graphene sheet and hence likely to give better accuracy in the estimated values, provided a proper method for simulation and proper parameters in the modeling are adopted.

An extensive review of the existing literatures on theoretical calculations shows wide diversity in the calculated values of Young's modulus and other mechanical properties of graphene. This is basically due to the difference in the prevailing parameters considered in the simulation by different authors. This necessitates a comprehensive study on the mechanical properties of graphene sheets and develops correlations between different mechanical properties and the prevailing parameters, like structure, size, temperature, strain rate and loading condition. Since direct experiment on individual graphene sheet, which is likely to give better accuracy on the measured values of the mechanical properties is formidable, simulation using suitable method is the alternative way to evaluate its mechanical properties and thus to design it for the targeted structural applications. Different ways can be adopted to evaluate the behavior of graphene under mechanical load, and from this the useful mechanical properties can be extracted. Molecular dynamics (MD)- and density functional theory (DFT)-based calculations seem to be very relevant for simulating the behavior and properties of graphene under mechanical loading.

The present work aims to make a detailed study on the mechanical properties of graphene using the MD-based modeling techniques. These atomistic modeling techniques are expected to give reasonable predictions in the case of nanoscale structure, like graphene, which is a two-dimensional nanostructure. For the proper application of graphene, there is a need for prior designing and the knowledge of mechanism and phenomenon inherent in it under different loading conditions. MD simulation technique, which is proved to be very powerful method (Ref 17) for the behavior and properties of nanostructured materials, has been taken up here to explore the mechanical properties of graphene.

2. Modeling Approaches

In the present study, four different approaches have been taken up for estimating the mechanical properties e.g., Young's modulus, yield strength, ductility, of a single-layer graphene sheet using MD simulations. These approaches are: tensile modeling, bending modeling, oscillation modeling and equilibrium MD modeling. Poisson's ratio has also been estimated based on the tensile modeling data in the elastic range. Before the execution of all the MD-based models, four single-layer graphene sheet samples of 700 Å length and 200 Å width have been generated and then these are thermally equilibrated at room temperature (298 K).

2.1 Thermal Equilibration

This is the initial sample preparation stage executed by MD technique. In the present work, all the MD simulations including the sample preparation (i.e., thermal equilibration) have been carried out using "LAMMPS" (Large-scale Atomic/Molecular Massively Parallel Simulator), the open-source MD simulation software package. First of all, four single-layer graphene sheet samples, each of 700 Å length and 200 A width, have been generated using a suitable crystal structure generation algorithm for 2D hexagonal structure without any lattice defect. After initializing the positions of carbon atoms in graphene, the velocities of the atoms are initialized according to Maxwell–Boltzmann distribution, as described in (Ref 18), corresponding to the target temperature of 298 K. The thermal equilibration process was run in NVT ensemble for 10,000 time steps of step size 1 fs, after initialization of both the position and velocity of the atoms within the graphene sheet. The Tersoff interatomic potential (Ref 19), which is considered to be suitable for all carbon-based materials, has been used in the present MD simulation algorithm for both thermal equilibration and the subsequent production stage. To advance the trajectories of the atoms of graphene sheet both during thermal equilibration and the subsequent production stage, the time integration has been carried out using Velocity-Verlet algorithm (Ref 20) with a time step size of 1 fs. During the thermal equilibration, Nose–Hoover thermostat (Ref 21) has been used to achieve the graphene sheet in the equilibrium condition at temperature within close tolerance to the target temperature (i.e., 298 K). The phase space of the graphene sheet (i.e., position and velocity of each and every atoms of the graphene sheet) with progress of time, which represents the dynamics of the atoms of the graphene sheet, is recorded at regular interval of time and based on this, the configuration of the sheet and its temperature are obtained during the process of thermal equilibration. The subsequent production stage, i.e., the stage for the evaluation of mechanical properties, starts from the phase space of the equilibrated graphene sheet.

In Fig. 1, the configuration of the graphene sheet both (A) before and (B) after equilibration and also the (C) fluctuation in temperature of the graphene sheet during equilibration has been shown. It is evident that there is some distortion of the sheet due to the equilibration process. It was found that due to the thermal equilibration the length decreases significantly, whereas the width increases somewhat, as compared to that before equilibration. This happens due to its thin 2D structure which causes some distortion in the sheet even for a small variation in the local temperature within the sheet during the equilibration process. However, this distortion has a negligible effect on the mechanical properties of the graphene sheet, because in the subsequent stage the sheet is subjected to a longitudinal stress which eliminates the distortion at the very beginning of loading and thus does not influence the mechanical properties like yield strength, Young's modulus, which are evaluated on the basis of the measurements done at relatively later stage of loading. The plot of average temperature of the graphene sheet with progress of time (Fig. 1c) has evidenced that the sheet has got thermally equilibrated with the final temperature within close tolerance (± 1 K) to the target temperature (298 K).

2.2 MD Simulations for the Evaluation of Mechanical Properties

After the thermal equilibration, the graphene sheets are subjected to different types of loading condition, viz., tensile, bending and oscillation, and from the response of the sheet under load the useful mechanical properties are extracted. These are non-equilibrium MD modeling executed under varying load or displacement in a given loading condition. In

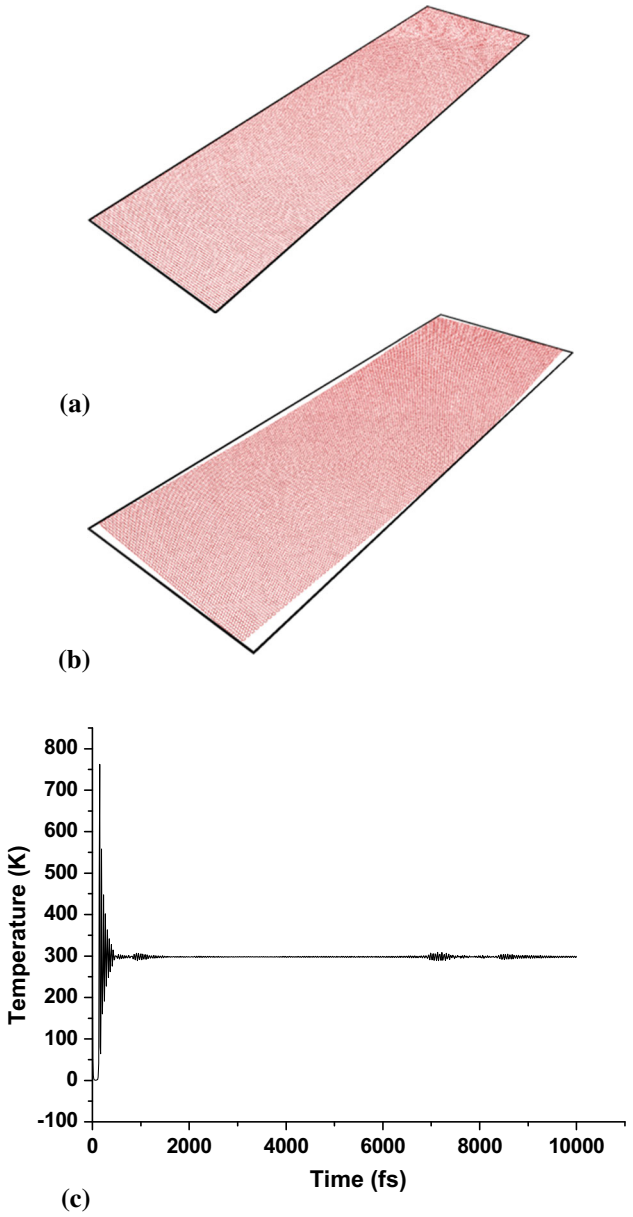

Fig. 1 Configuration of the graphene sheet (a) before and (b) after equilibration; and the (c) average temperature of the graphene sheet with progress of time during the thermal equilibration

one approach, equilibrium MD simulation has been carried out at varying edge length of the unit cell of graphene and the potential energy has been estimated at each edge length. Based on the potential energy versus edge length data, the mechanical properties have been estimated. All the above non-equilibrium MD techniques have been performed using NVE ensemble. This is the actual production stage wherefrom the mechanical properties of the graphene sheet are evaluated. This stage is executed using the same Tersoff interatomic potential, as used during the equilibration stage, for atomic interactions within the graphene sheet and the Velocity-Verlet algorithm with a time step size of 1 fs has been used for time integration. In the actual production stage when the graphene sheet is subjected to external forcing in non-equilibrium methods, the total energy is conserved and hence NVE ensemble is used in these simulations. The calculation in equilibrium MD method is based on the consideration of NVT ensemble. Hence, in all the instances of non-equilibrium MD methods, NVE ensemble has been used in the production stage. However, in the prior equilibration stage which is the sample preparation stage the graphene sheet is thermostatted using Nose–Hoover thermostat. This necessitates the use of NVT ensemble for achieving thermal equilibration. The number of runs of MD simulation is different for different methods. In the tensile modeling, five MD runs were carried out at five different strain rates and then the results were extrapolated to estimate the values of the mechanical properties. In both bending and oscillation methods, only one run was carried out in each case and hence the results obtained in these methods would have the overlapping effects of strain rate. In EMD method, a series of MD runs was carried out corresponding to different edge length (within the range from 2 to 4.5 Å) of the hexagonal unit cell of graphene using NVT ensemble and the results have been analyzed to estimate various mechanical properties. The individual MD modeling-based approaches for the evaluation of mechanical properties of the graphene sheet are detailed below:

2.2.1 Tensile Modeling. The equilibrated graphene sheet is subjected to tensile stretching in the longitudinal direction in a displacement-controlled manner at a constant displacement velocity of 1 Å/ps (engineering strain rate = 2.53×10^9 s^{-1}). For this, the graphene sheet is divided into three parts along the longitudinal direction: one end part of length 106 Å is kept fixed, the other end part of length 106 Å is made to move at a constant velocity (1 Å/ps) and the middle part of length 396 A deforms under tensile loading. The atoms in the moving end are made to displace by a distance of 0.001 Å in each time step of 1 fs continuously in a coordinated fashion away from the other fixed end, wherein the atoms are kept fixed in their as-equilibrated position. The middle portion of the sheet is allowed to deform in response of tensile loading. The loading condition of the graphene sheet considered in the present tensile modeling is schematically shown in Fig. 2. During this process of tensile loading, all the atoms are allowed to interact among themselves by means of the Tersoff interaction potential, but while updating their position, the atoms at the fixed end are kept fixed at their as-equilibrated position, the atoms at the moving end are displaced by 0.001 Å in each time step (of 1 fs) along the longitudinal direction away from the fixed end, and the position of the atoms at the middle portion is updated as per the interaction forces they experience from the surrounding atoms. While the moving end is displaced monotonically, the net force resulted at the fixed end has been calculated in each step by summing up the force component in the longitudinal direction of all the atoms in the fixed end. This net force at any given moment divided by the original cross-sectional area (95.62795 $Å^2$ in this case) gives the engineering stress at that moment. The corresponding engineering strain is calculated by dividing the longitudinal displacement of center of mass position of the moving end with respect to the as-equilibrated condition, by the initial gauge length (396 Å) of the sheet after equilibration. Thus, in the present tensile model the strain to the sheet is provided in the longitudinal direction at a constant strain rate by displacing the moving end at a constant rate, and the resultant stress at the fixed end has been tracked with increase in strain. The stress versus strain plot thus obtained can be analyzed to extract the useful mechanical properties, viz. Young's modulus, yield strength and percent elongation. The phase space has been tracked regularly, and the configuration of

the graphene sheet obtained there from has been linked with the stress–strain curve of the sheet at different points of time of the tensile loading. Additionally, the temperature of the deformable portion at the middle of the sheet has been tracked with progress of deformation to get an idea about the thermal effect associated with the tensile deformation of a graphene sheet. Thus, in the present study, the tensile model of a graphene sheet has been framed in a way analogous to the real experimental process of tensile testing of bulk specimen. However, in the model the strain rate used is several orders of magnitude higher than that used in the real experiments. This is done to keep the computation time within a manageable limit. To cope up with the ultra-high strain rate that may cause some error in the estimated values of the mechanical properties, the strain rate has been varied within a range by three orders of magnitude and the estimated values of mechanical properties are extrapolated to the low strain rate side that is used in the real experimental measurement.

It is to be noted here that calculation of engineering stress requires the value of thickness of graphene sheet. Microscopically, a single-layer graphene sheet is severely undulated. The effective thickness (h) has been calculated by the following equation:

$$h = \frac{nV}{lb} \qquad \text{(Eq 1)}$$

where n, V, l and b are number of atoms (46150) in the graphene sheet, volume of each atom (1.25983 Å^3) in the graphene sheet, length and width of the graphene sheet after equilibration, respectively. The effective thickness thus calculated is multiplied by the width (after equilibration) to get the original (initial) cross-sectional area of the sheet.

To calculate the Poisson's ratio on the basis of tensile modeling data of graphene sheet, the length and width of a preselected portion at the middle within the deformable region of the sheet are estimated at different instances and then the Poisson's ratio has been calculated at those instances of loading with respect to that at the equilibrated (at 298 K) condition, using the following equation:

$$\vartheta = \frac{\frac{\Delta b_s}{b_s}}{\frac{\Delta l_s}{l_s}} \qquad \text{(Eq 2)}$$

where b_s and l_s represent width and length of the preselected middle portion of the graphene sheet and Δb_s and Δl_s represent change in width and change in length of the same preselected middle portion of the graphene sheet with respect to those after equilibration, respectively, due to tensile stretching. In the present work, the Poisson's ratio values are calculated at three different instances after the start of tensile loading, viz. 40,000, 50,000 and 60,000 time steps of 1 fs and corresponding to those time steps the values of Poisson's ratio are calculated (using Eq 2) and then averaged out to get the average Poisson's ratio value of the graphene sheet. This is an important mechanical property estimated in this way, and this value is used where ever needed in the present study.

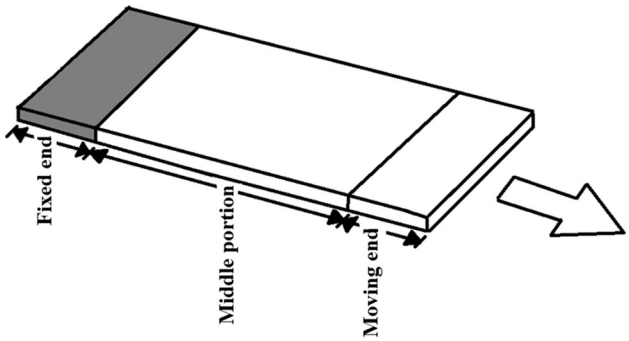

Fig. 2 Schematic drawing depicting the loading condition of graphene sheet, considered in tensile modeling

2.2.2 Bending Modeling. In bending modeling, the equilibrated graphene sheet is initially kept horizontally, as shown schematically in Fig. 3. In this case, the two end parts of the sheet are kept fixed, and within the middle portion a small band of width 28.3 Å perpendicular to the longitudinal axis is selected at the center. This portion at the center of the sheet is subjected to a monotonically increasing force, at a rate of 0.1 eV/Å (=1.60218×10^{-10} N) per time step of 1 fs, in the downward direction and allowed the middle portion of the graphene sheet to deflect gradually. In that sense, the present bending model is representative of a load-controlled deformation process. The extent of deflection at any instance depends on the force applied at the center band. Figure 3 shows schematically the graphene sheet at a given instance of bending loading. It is obvious that in this type of loading also the middle portion of the sheet is subjected to stretching in the longitudinal direction and the longitudinal strain resulted at any point of time is dependent on the load applied at that point of time in the downward direction. Based on the load applied and the resultant deflection, the longitudinal stress and strain both can be calculated out.

Let us suppose, in the initial unloaded condition the length of the middle portion of the graphene sheet is l_e. The sheet is subjected to bending type of loading in the downward direction, and it increases continuously at a constant rate to make the sheet deflect more and more. Suppose, at a load value of F_1 the deflection caused is l_d at the central band of the sheet. The part of the sheet (OB) with an initial length of $l_e/2$ has been stretched to a length of l_p ($l_p > l_e/2$), as shown in Fig. 3, under the transverse load of F_1, applied at the central band of the sheet. This applied force F_1 gets balanced by two other resultant tensile forces, F_2 and F_3, which act in the longitudinal direction within the stretched (deflected) parts, O′B and O′A, respectively. Since, O′A = O′B, so $F_2 = F_3 = F$ (say). Suppose, the included angles are α, β and γ, respectively. Therefore, under this loading condition:

$$l_p = \sqrt{\frac{1}{4}l_e^2 + l_d^2}. \qquad \text{(Eq 3)}$$

In the above equation, l_e is known. The value of l_d at any instance of loading can be obtained on the basis of displacement of the center of mass position of the central band in downward direction with respect to the initial unloaded

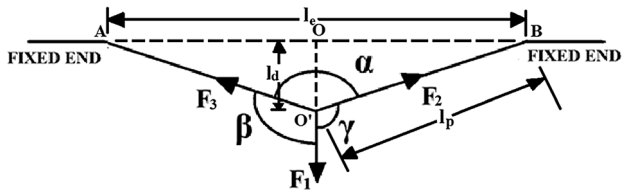

Fig. 3 Schematic drawing representing the loading condition of graphene sheet, considered in bending modeling

condition. Thus, l_p can be calculated out and from the calculated value of l_p the longitudinal strain can be evaluated from Eq 4:

$$\text{Strain} = \frac{l_p - \frac{1}{2}l_e}{\frac{1}{2}l_e}. \quad \text{(Eq 4)}$$

When the system is in equilibrium under three loads, viz. F_1, F_2 and F_3, the Lami's theorem can be applied. Here, $F_2 = F_3 = F$ (longitudinal force) and $\beta = \gamma = 180° - \alpha/2$. Hence, from the Lami's theorem the longitudinal force, F can be calculated, having known the applied (transverse) force F_1, based on the following equation:

$$F = \frac{F_1}{2\cos\frac{\alpha}{2}} = \frac{F_1}{2\frac{l_d}{l_p}}. \quad \text{(Eq 5)}$$

From the longitudinal force the corresponding value of longitudinal (engineering) stress can be calculated out, by dividing the force by the original area of cross section of the sheet, on the basis of the following equation:

$$\text{Stress} = \frac{F}{bh}. \quad \text{(Eq 6)}$$

From Eq 4 and 6, a database of engineering strain and the corresponding engineering stress are generated on the basis of resultant displacement of the central band of the sheet (l_d) and the applied transverse load (F_1), both of which are estimated by the MD simulation with progress of the loading of the graphene sheet under bending condition. The slope of the linear portion of the longitudinal stress versus strain curve gives the Young's modulus under the bending type of loading condition.

2.2.3 Oscillation Modeling. In oscillation modeling, the equilibrated graphene sheet is first subjected to transverse loading when the two ends are kept fixed, as in bending modeling, and made the central band of the sheet to deflect (displace) by 64 Å with respect to the (initially) horizontally placed unloaded sheet. Thereafter, the load is released abruptly and the middle portion of the sheet is allowed to rebound and oscillate. This oscillation phenomenon of the sheet subsequent to the plucking process has been tracked by means of the displacement (in the vertical direction) of the center of mass position of the central band with respect to that in the fully loaded condition (just before plucking), with progress of time. From the slope of the initial portion of the displacement versus time plot, the rebound velocity ($\dot{z}_0$) at time $t = 0$ has been evaluated and using its value the natural angular frequency (ω_n) for undamped oscillation has been estimated, on the basis of the following equation (Ref 22):

$$\omega_n = \frac{\dot{z}_0}{A_0} \quad \text{(Eq 7)}$$

where A_0 is the amplitude for undamped oscillation (=64 Å in the present simulation). Although it is likely that after plucking the graphene sheet would undergo damped oscillation as a whole, but the initial rebound velocity can be estimated based on the present model to get the value of natural frequency, i.e., the frequency of oscillation had the sheet been undergone undamped oscillation. Using the value of ω_n the in-plane Young's modulus (E) of the graphene sheet has been estimated from the following equation (Ref 22):

$$E = \frac{\omega_n^2 m}{h} \quad \text{(Eq 8)}$$

where m is the mass of the sheet.

2.2.4 Equilibrium MD Modeling. All the above three MD approaches are non-equilibrium MD methods (NEMD). Apart from these, equilibrium MD simulations (EMD) have also been carried out with an aim to evaluate the mechanical properties of graphene sheet. In this EMD method, a series of MD simulations have been carried out at room temperature (298 K) for varying edge length (a) of the unit cell of non-equilibrated graphene sheet, using NVT ensemble and corresponding to each edge length the potential energy has been estimated. The minimum value of the potential energy per atom of the graphene sheet determined from a plot of per atom potential energy versus edge length is the cohesive energy, and the corresponding value of edge length is the equilibrium lattice parameter (a_0). The bulk modulus (B) has been calculated from the curvature of the same plot at the point of minimum potential energy, using the following equation (Ref 23):

$$B = \frac{a_0^2}{9V_0'}\frac{d^2U}{da^2}\bigg|_{a=a_0} \quad \text{(Eq 9)}$$

where U is the potential energy per atom and V_0' is the equilibrium volume per atom. From the value of bulk modulus, the Young's modulus of the graphene sheet has been calculated on the basis of the following general equation:

$$E = 3B(1 - 2\vartheta). \quad \text{(Eq 10)}$$

The value of ϑ (Poisson's ratio) is taken from the prior tensile model-based calculations.

3. Results and Discussion

The tensile model for graphene sheet, which was framed mimicking the real tensile test experiment of bulk sheet materials, uses an ultra-high strain rate. Such a strain rate, although not achievable in real experiments, has been used here because of the limitations in the computation power. Naturally, the mechanical properties evaluated under an ultra-high strain rate will have an effect of the strain rate and cannot be compared with the available experimental data which were obtained under slow strain rate condition in tensile testing. Thus, the results of present tensile model will represent the behavior and properties of graphene sheet under ultra-high strain rate tensile loading condition. Extrapolation of the data at varying strain rate, to low strain rate side would likely to eliminate the strain rate effect and give the approximate values of mechanical properties of graphene sheet, corresponding to conventional low strain rate. However, this exercise would yield an approximate result and so it is better to avoid it retaining the data evaluated under ultra-high strain rate. Thus, the present tensile model is aimed to investigate the mechanical behavior of graphene sheet under ultra-high strain rate and extract mechanical properties there from.

Figure 4 displays the engineering stress-strain curve evaluated on the basis of present tensile model of graphene sheet at a strain rate of 2.53×10^9 s^{-1}. The fluctuation of the stress value with increase in strain is typical of any MD simulation data for nano-sized particles. The smoothed plot shows an

initial linear elastic part rising continuously up to a maximum value, followed by rapid fall offof the stress with strain until the stress becomes zero. In contrast to the bulk materials, the present engineering stress–strain plot does not show nonlinear plastic region representing uniform plastic deformation. The maximum value of the engineering stress is the yield strength which is same as the tensile strength of the graphene sheet, because both the parameters merge under ultra-high strain rate tensile loading condition. The slope of the initial linear elastic part is the Young's modulus, and the value of strain at which the stress becomes zero after the yield point is the %elongation, if the strain is represented in percentage. The mechanical properties extracted from Fig. 4 are presented in Table 1. It is obvious that the graphene sheet, under ultra-high tensile deformation, exhibits yield strength much higher than that of the conventional bulk materials, and its Young's modulus is several orders of magnitude greater than that of the conventional bulk materials. In fact, the results show that the graphene sheet has the highest in-plane strength evaluated under ultra-high strain rate tensile loading. Figure 4 also shows the variation in temperature of the middle portion of the sheet during the process of ultra-high strain rate tensile deformation. At the very beginning of the deformation process, the temperature rises to ~457 K and remains almost constant at that value with further progress of deformation. The temperature rise is a natural consequence of the plastic deformation process. However, in the present case the rise in temperature is very high, which is due to the typical 2D nanostructure of the graphene sheet and its very high specific surface area.

In Fig. 5, the progressive stages of tensile deformation of the graphene sheet have been presented in terms of the configuration plots at different instances of loading until fracture. It is evident that the present displacement-controlled tensile deformation process initially results gradual thinning down of the middle portion of the sheet. This is followed by the failure process consisting of initiation of a crack at an edge of the sheet and its subsequent propagation across the width until complete fracture occurs. The configuration plots presented in Fig. 5 have evidenced a link with the engineering stress–strain curve shown earlier. It is found that within the linear elastic region the progressive thinning down of the sheet occurs. At the yield point, the crack initiates and subsequently it (crack) propagates until the sheet fractures into two pieces, at the point of time when the stress drops down to zero.

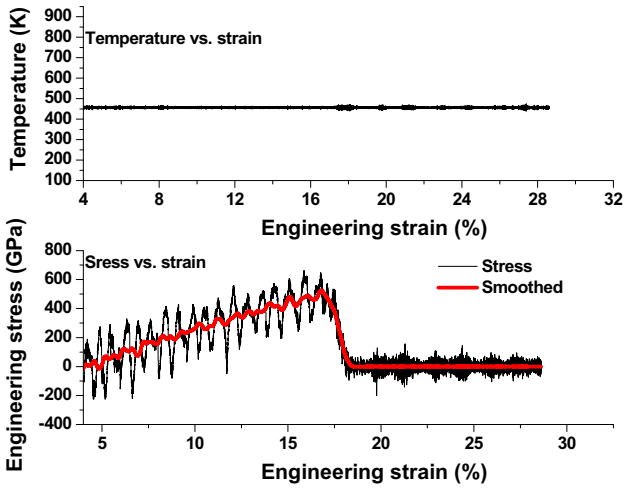

Fig. 4 Engineering stress–strain curve, along with the thermal effect evaluated by tensile modeling of graphene sheet

The Poisson's ratio has been calculated on the basis of change in length and width of a preselected portion of the graphene sheet during the stage of linear elastic deformation under tensile loading. The values of length and width of the preselected portion of the sheet at different points of time during the tensile loading, along with those immediately after equilibration, have been presented in Table 2. The average value of Poisson's ratio of the graphene sheet comes out to be 0.23 under in-plane tensile loading condition. This value of Poisson's ratio is much less compared to that of the conventional bulk materials.

The bend stretching model wherein the transverse load has been applied to cause in-plane stretching to the graphene sheet fixed at two ends also represents tensile behavior of the sheet. The in-plane engineering stress–strain curve determined under such a loading condition has been shown in Fig. 6. It is evident that after some initial nonlinear part, the engineering stress–strain plot shows linearity. The initial part is nonlinear and mostly with increasing slope, because of the gradual increase in the part being deflected of the graphene sheet within the middle portion with respect to the initial unloaded position at the initial stage of loading. Once the entire middle portion of the sheet is deflected, the in-plane stress starts developing in a linear fashion and the sheet behaves like a linear elastic material. The slope of this linear portion of the engineering stress–strain curve determined under primary bend loading is the Young's modulus and has been estimated to be 5.5812 TPa (Table 1). It is to be noted here that this value of Young's modulus also corresponds to ultra-high strain rate deformation and hence includes the strain rate effect. In this case, the applied in-plane strain rate is 13.1×10^9 s^{-1}, which is more than five times the strain rate applied in the tensile modeling. The higher value of strain rate applied in bending modeling has caused higher value of Young's modulus as compared to that calculated on the basis of earlier tensile modeling. This finding supports the strain rate effect of the mechanical properties of graphene sheet. The configuration of the graphene sheet at different stages of bend loading has been presented in Fig. 7. This reveals perfectly flat sheet at the initial unloaded condition, partly deflected configuration at some intermediate stage of loading when there is nonlinearity in the stress–strain behavior, and fully deflected sheet (middle portion) at the final stage of loading. In the present work, a good correlation is found between the macroscopic stress–strain behavior and the configuration plots representing microstate at different stages of bend loading of the graphene sheet.

The present bending model has been designed mimicking the experimental test for the determination of Young's modulus of nanowires or such kind of nanoscale structures using atomic force microscope (AFM) tip. There are several reports on this type of experimental study and are well established (Ref 24-27). Determination of Young's modulus of nanoscale materials under bending loading is a convenient experimental method and hence has been adopted in several studies (Ref 24-27). The aforesaid experimental method has been mimicked here in a molecular dynamic-based model, which theoretically evaluates the stress–strain response of a graphene sheet under bending load and based on this the Young's modulus has been estimated. In that sense, there is nothing wrong with the present model. However, due to limitation in computation speed the loading rate was made several orders of magnitude higher than that

Table 1 The values of different mechanical and physical properties estimated by different modeling approaches adopted in the present work on graphene sheet

Sr. no.	Method	Young's modulus, TPa	Bulk modulus, TPa	Yield strength, GPa	% Elongation	Cohesive energy, eV/atom	Poisson's ratio
1.	Tensile	3.8976	…	507	18%	…	0.23
2.	Bending	5.5812	…	…	…	…	…
3.	Oscillation	1.5237	…	…	…	…	…
4.	Equilibrium MD	0.7209	0.4449	…	…	−3.4622	…

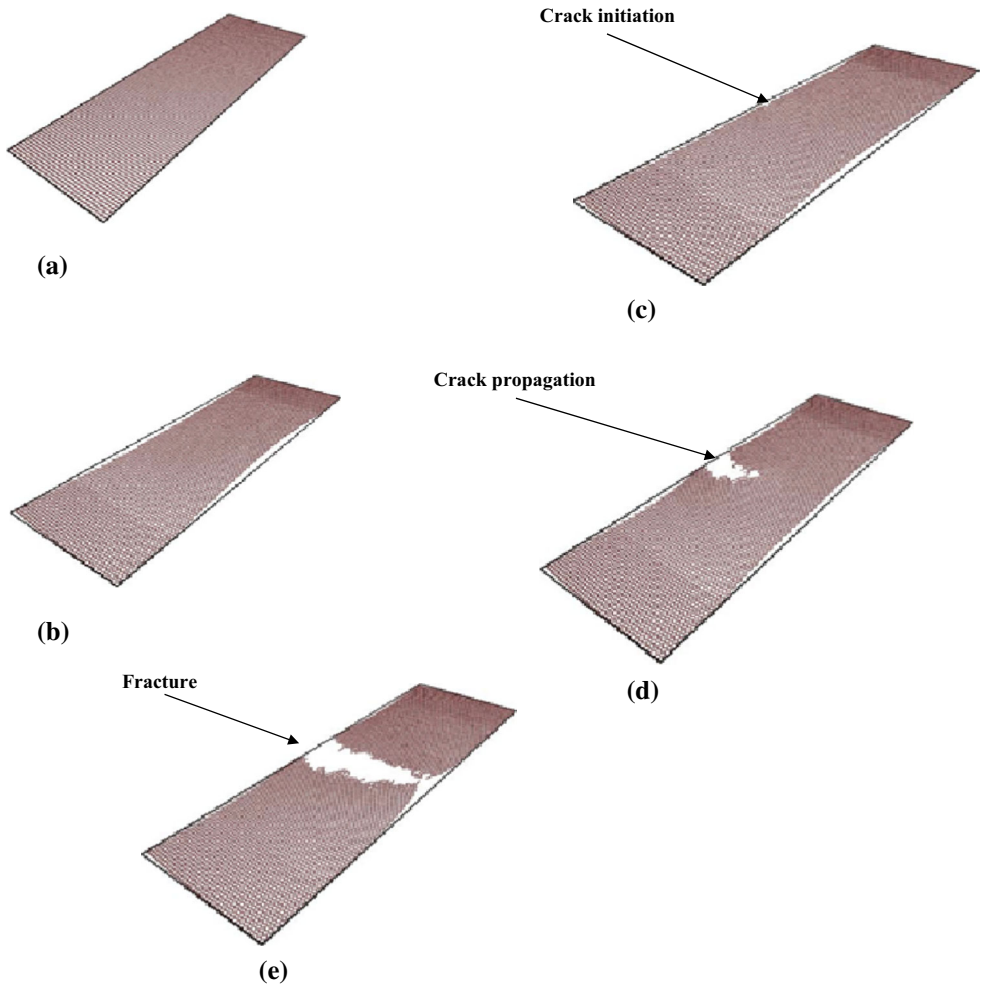

Fig. 5 The configuration at progressive stages of tensile deformation of graphene sheet under ultra-high strain rate: (a) initial; (b) deformed elastically; (c) initiation of crack; (d) propagation of crack; and (e) complete fracture

Table 2 Length and width of a preselected portion of the graphene sheet at different points of time during the stage of linear elastic deformation under tensile loading and the corresponding values of Poisson's ratio

No. of time steps of 1 fs during deformation after equilibration	Length, Å	Width, Å	Calculated value of Poisson's ratio	Average value of Poisson's ratio
0	366.936	208.9500	…	0.23
40,000	406.839	204.0905	0.2138	
50000	416.814	203.3188	0.1982	
60000	426.567	199.5395	0.2771	

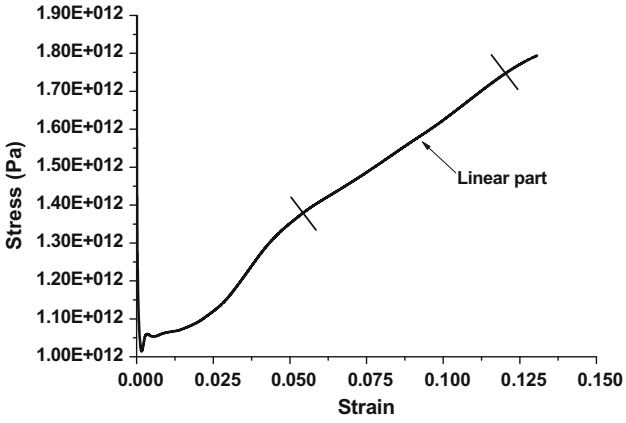

Fig. 6 Engineering stress–strain curve determined from bending modeling

applied in real experiments. This has resulted in a higher value of Young's modulus of graphene sheet than that obtained experimentally. Had the loading rate/strain rate effect in the bending modeling been decoupled in the theoretical estimation, which is a formidable task in the context of MD simulation, the calculated value would have matched with the experimentally determined value. Nevertheless, the present scheme provides a useful guideline for the estimation of Young's modulus of graphene sheet under ultra-high rate bending loading.

The oscillation modeling of graphene sheet aims to determine the natural frequency of oscillation after the sheet, which is fixed at the two ends, is plucked at the central band by the application of some load in the transverse direction. The displacement of the center of mass of the central band in vertical direction with respect to that in the fully loaded condition, with progress of time after plucking, has been displayed in Fig. 8. It is apparent that immediately after the sheet is plucked it rebounds at a constant linear velocity of 562.7 m/s. Thereafter, the velocity of rebound is found to vary in a nonlinear fashion and on a whole it (velocity) decreases with time. The initial constant rebound velocity has been determined from the slope of the initial linear part of the displacement versus time curve, shown in Fig. 8. On the basis of this initial rebound velocity, the natural angular frequency has been estimated from Eq 7 and it comes out to be 87.9×10^9 rad/s. The Young's modulus calculated using the estimated value of natural angular frequency is found to be 1.5237 TPa. This value is somewhat less compared to that estimated using tensile modeling and bending modeling. This is expected, because in the oscillation modeling there is no overlapping effect of strain rate that prevails in the earlier tensile modeling and bending modeling. Figure 9 shows the configuration of the graphene sheet during the process of rebound after plucking, along with that before plucking, i.e., during loading prior to plucking.

The potential energy per atom of graphene sheet has been calculated using equilibrium MD method at temperature 298 K (room temperature) considering NVT ensemble and it is tabulated for a series of assumed edge length of the unit cell of the sheet. The graphical representation of the potential energy per atom of graphene sheet with varying edge length has

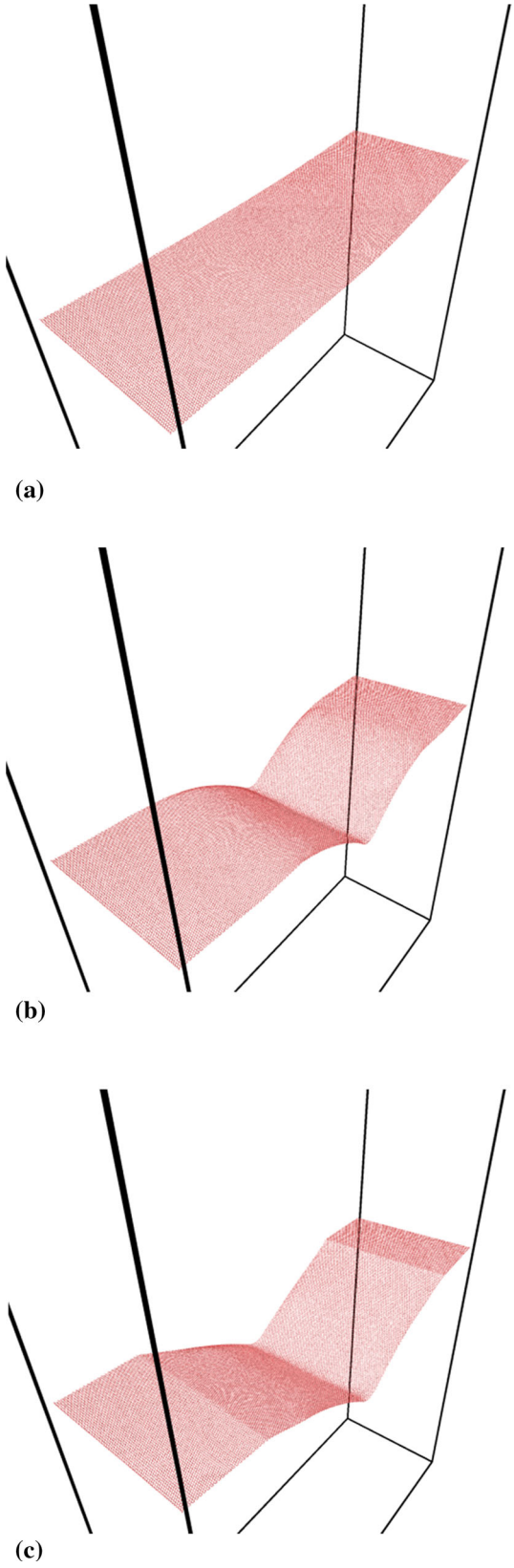

Fig. 7 Configuration of the graphene sheet at different stages of bend stretching: (a) initial; (b) intermediate; and (c) final

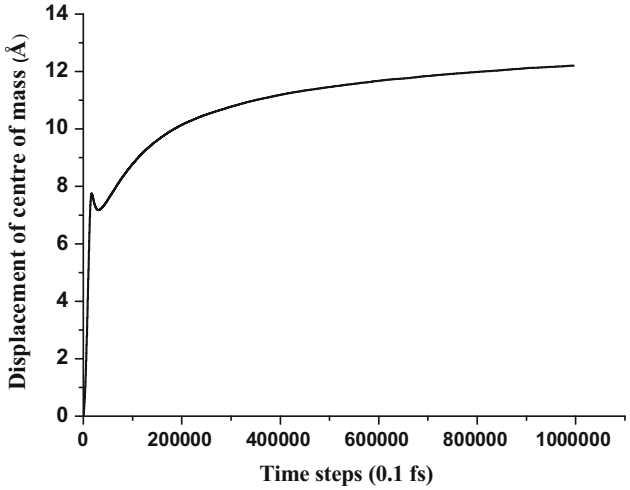

Fig. 8 Displacement of center of mass of the central band of graphene sheet with progress of time after plucking

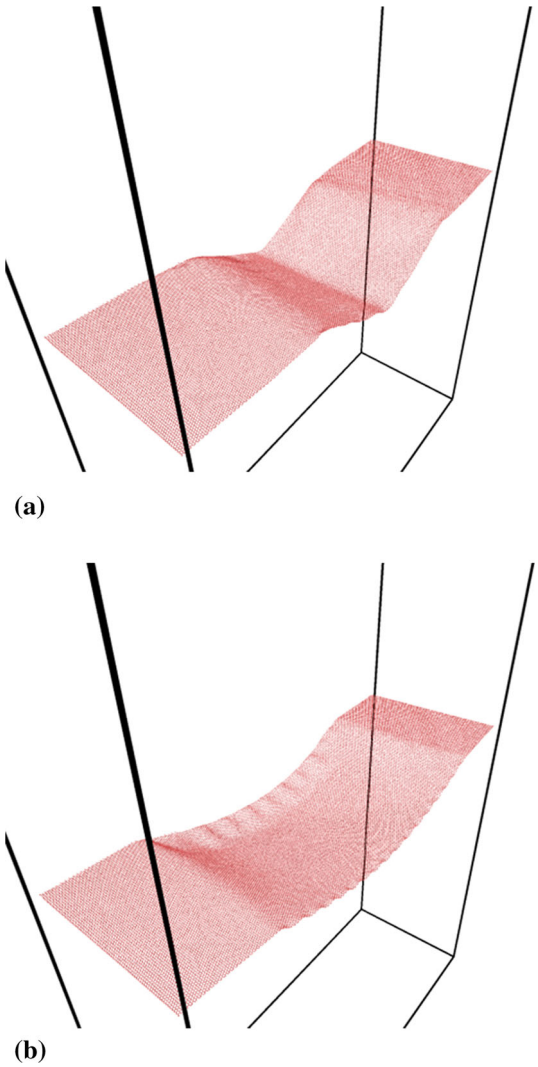

Fig. 9 Configuration of the graphene sheet (a) before plucking and (b) at some intermediate stage during rebounding process

been displayed in Fig. 10(a). The equilibrium lattice parameter and cohesive energy estimated on the basis of Fig. 10(a) are found to be 2.6 Å and −3.4622 eV/atom, respectively (Table 1). In order to calculate the bulk modulus of the graphene sheet determination of curvature of the potential energy per atom versus edge length plot at the point of minimum potential energy is required. For this, a second plot is made by differentiation of the data points of Fig. 10(a) and is presented as Fig. 10(b) representing the variation of force per atom in graphene sheet as a function of edge length. The slope of force per atom versus edge length plot (Fig. 10b) at the point of minimum potential energy (or zero force) gives the value of curvature and it comes out to be 22.83713 eV/Å^2. The calculated value of bulk modulus of graphene sheet using this value of curvature in Eq 9 is 0.4449 TPa and its corresponding value of Young's modulus is 0.7209 TPa (Table 1). It is noteworthy that the value of Young's modulus determined by the present equilibrium MD method is less compared to other non-equilibrium methods described previously. This is expected, since this method of calculation is done under equilibrium condition and does not involve any external forcing factor. Young's modulus of graphene sheet is very

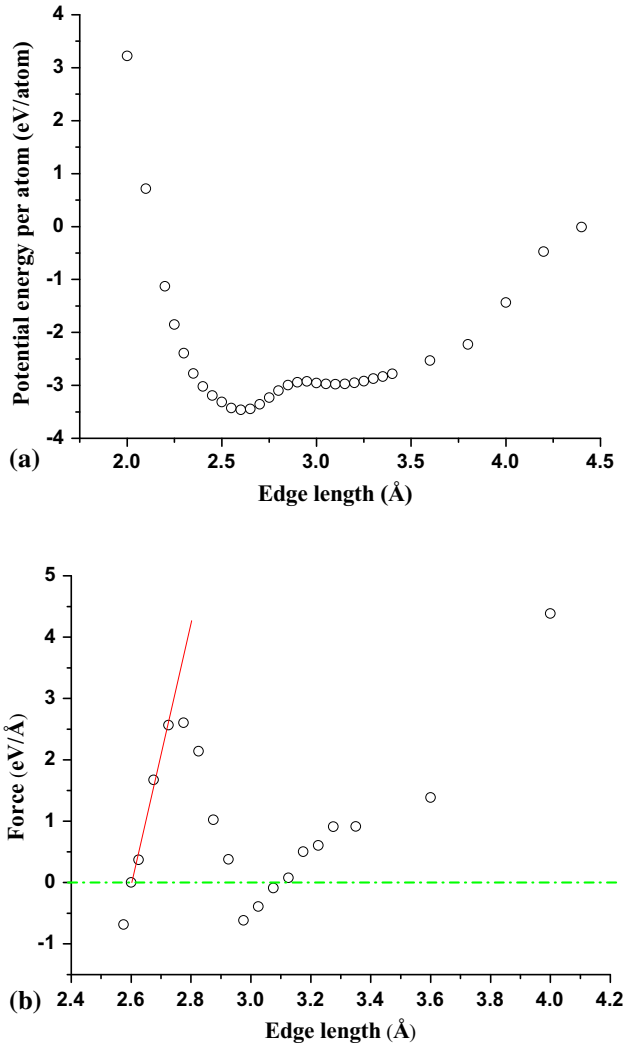

Fig. 10 Variation of (a) potential energy per atom and (b) force per atom, as a function of edge length of unit cell of single-layer graphene sheet

sensitive to strain rate. In the present simulations, the strain rate involved in various NEMD methods is different. The method with higher strain rate has given rise to the higher value of Young's modulus as compared to those involving lower strain rate. This is expected based on the principle of deformation of materials under various loading conditions. Faster rate of deformation leads to incomplete relaxation of the structure and hence gives rise to higher value of modulus. In the equilibrium MD method, external forcing factor is completely absent. Hence, the value of Young's modulus estimated on the basis of EMD method is less, as compared to those involving external forcing factor applied at high strain rate.

There are diversities in the estimated values of Young's modulus depending upon the method adopted in the present work. However, as a whole, the present work on graphene sheet which explores the mechanical properties using various MD-based approaches establishes that the graphene is several orders of magnitude stronger than other conventional materials and so it (graphene) can potentially be used in advanced applications where ultra-high strength is required. The main focus of the present study is to use MD simulation tool to estimate the mechanical properties of graphene sheet under various non-equilibrium loading conditions and also equilibrium condition. Accordingly, the estimated values are different in different approaches. This mismatch is quite natural considering the wide difference in the loading rate/strain rate used in different non-equilibrium MD approaches. Thus, the diversity in the results has been explained here in terms of the physical laws. The best way to deal with this matter and to remove confusion is to report the present estimated values with proper mention of the corresponding condition of loading rate/strain rate under which simulation was carried out. The objective here is not to supersede the experimental technique, but to obtain atomic level understanding of the mechanical behavior of the graphene sheet under various prevailing conditions and to extract relevant mechanical properties there from.

It is to be noted here that the present article has focused on molecular dynamic-based various approaches for the estimation of mechanical properties of graphene sheet. The results obtained in those methods have been compared and explained in terms of the known laws of physics. A rigorous study has been reported here for the estimation of mechanical properties of graphene sheet using the methods like tensile, bending, oscillation and equilibrium molecular dynamics. The work is indeed novel and unattempted in the existing literature. All the four methods reported in the present article have not been attempted previously. People have evaluated the mechanical properties of graphene sheet by some other methods. However, the methods adopted here are new and thus the present work is an improvement upon the state-of-the-art.

4. Conclusions

Mechanical properties, for example, Young's modulus, yield strength, %elongation and Poisson's ratio of graphene sheet have been evaluated with the help of MD simulation-based four different approaches, viz. tensile modeling, bending modeling, oscillation modeling and equilibrium MD modeling. Although there are diversities in the values of Young's modulus estimated by these methods, but, as a whole, the present work establishes the ultra-high strength of individual graphene sheet. The diversity arises mainly due to strain rate or external force factor effects. These methods which have been explored here were not attempted previously for graphene sheet and can be useful for mechanical design of graphene- or graphene-based materials.

Acknowledgments

The financial support of the Center of Excellence (CoE) Grant under TEQIP-II is thankfully acknowledged.

References

1. S. Maity and M. Ganguly, *Elements of Chemistry*, 6th ed., Publishing Syndicate, Kolkata, 2003, p 52–69
2. Z. Qi, D.K. Campbell, and H.S. Park, Atomistic Simulations of Tension-Induced Large Deformation and Stretchability in Graphene Kirigami, *Phys. Rev. B*, 2014, **90**, p 245437-1–245437-7
3. C.L.P. Pavihtra, B.V. Sarada, K.V. Rajulapati, T.N. Rao, and G. Sundararajan, A new Electrochemical Approach for the Synthesis of Copper–Graphene Nanocomposite Foils with High Hardness, *Sci. Rep.*, 2014, **4**(4049), p 1–7
4. K. Jagannadham, Thermal Conductivity of Copper–Graphene Composite Films Synthesized by Electrochemical Deposition with Exfoliated Graphene Platelets, *Metall. Mater. Trans. B*, 2012, **43**, p 316–324
5. http://www.bbc.co.uk/news/science-environment-21025686, 2013, Accessed 15 January 2013, Source: BBC News
6. A. Lavoisier, Traite Elementire de Chimie (Elementary Treatise of Chemistry), A Paris, Chez Cuchet, 1789, p 1–35 **(in French)**
7. A.K. Geim and K.S. Novoselov, The Rise of Graphene, *Nat. Mater.*, 2007, **6**, p 183–191
8. K.S. Novoselov, V.I. Fal'ko, L. Colombo, P.R. Gellert, M.G. Schwab, and K. Kim, A Roadmap for Graphene, *Nature*, 2012, **490**, p 192–200
9. C. Lee, X. Wei, J.W. Kysar, and J. Hone, Measurement of the Elastic Properties and Intrinsic Strength of Monolayer Graphene, *Science*, 2008, **321**, p 385–388
10. J.U. Lee, D. Yoon, and H. Cheong, Estimation of Young's Modulus of Graphene by Raman Spectroscopy, *Nano Lett.*, 2012, **12**, p 4444–4448
11. http://news.yahoo.com/5-ways-graphene-change-gadgets-155243022.html, 2014, Accessed 14 April 2014, Source: Yahoo News
12. G. Cao, Atomistic Studies of Mechanical Properties of Graphene, *Polymer*, 2014, **6**, p 2404–2432
13. F. Liu, P. Ming, and J. Li, Ab Initio Calculation of Ideal Strength and Phonon Instability of Graphene in Tension, *Phys. Rev. B*, 2007, **76**, p 064120-1–064120-7
14. E. Konstantinova, S.O. Dantas, and P.M.V.B. Barone, Electronic and Elastic Properties of Two-Dimensional Carbon Planes, *Phys. Rev. B*, 2006, **74**, p 035417-1–035417-16
15. B. Hajgato, S. Guryel, Y. Dauphin, J.M. Blairon, H.E. Miltner, G.V. Lier, F.D. Proft, and P. Geerlings, Theoretical Investigation of the Intrinsic Mechanical Properties of Single- and Double-Layer Graphene, *J. Phys. Chem. C*, 2012, **116**, p 22608–22618
16. S.S. Gupta and R.C. Batra, Elastic Properties and Frequencies of Free Vibrations of Single-Layer Graphene Sheets, *J. Comput. Theor. Nanosci.*, 2010, **7**, p 1–14
17. L.V. Zhigilei, A.N. Volkov, and A.M. Dongare, Computational Study of Nanomaterials: From Large-Scale Atomistic Simulations to Mesoscopic Modelling, *Encyclopedia of Nanotechnology*, B. Bhushan, Ed., Springer, Heidelberg, 2012, p 470–480
18. A. Das and M.M. Ghosh, MD Simulation-Based Study on the Melting and Thermal Expansion Behaviors of Nanoparticles Under Heat Load, *Comput. Mater. Sci.*, 2015, **101**, p 88–95
19. J. Tersoff, New Empirical Approach for the Structure and Energy of Covalent Systems, *Phys. Rev. B*, 1988, **37**, p 6991–7000
20. J. Li, Basic Molecular Dynamics, *Handbook of Materials Modeling*, S. Yip, Ed., Springer, Dordrecht, 2005, p 565–588
21. D.J. Evans and B.L. Holian, The Nose-Hoover Thermostat, *J. Chem. Phys.*, 1985, **83**, p 4069–4074
22. D. Nag, *Mechanical Vibrations*, Wiley India Pvt. Ltd., New Delhi, 2011, p 31–48

23. J.G. Lee, *Computational Materials Science: An Introduction*, CRC Press (Taylor & Francis Group), Boca Raton, 2012, p 40
24. B. Wu, A. Heidelberg, and J.J. Boland, Mechanical Properties of Ultrahigh-strength Gold Nanowires, *Nat. Mater.*, 2005, **4**, p 525–529
25. T. Namazu, Y. Isono, and T. Tanaka, Evaluation of Size Effect on Mechanical Properties of Single Crystal Silicon by Nanoscale Bending Test Using AFM, *J. Microelectromech. Syst.*, 2000, **9**, p 450–459
26. S. Sundararajan and B. Bhushan, Development of AFM-based Techniques to Measure Mechanical Properties of Nanoscale Structures, *Sens. Actuators A Phys.*, 2002, **101**, p 338–351
27. H. Ni and X. Li, Young's Modulus of ZnO Nanobelts Measured Using Atomic Force Microscopy and Nanoindentation Techniques, *Nanotechnology*, 2006, **17**, p 3591–3597